JACS
JOURNAL OF THE AMERICAN CHEMICAL SOCIETY
Article
pubs.acs.org/JACS

Rotational Dynamics of Diazabicyclo[2.2.2]octane in Isomorphous Halogen-Bonded Co-crystals: Entropic and Enthalpic Effects

Luca Catalano,[†,‡] Salvador Perez-Estrada,[†] Hsin-Hua Wang,[§] Anoklase J.-L. Ayitou,[†] Saeed I. Khan,[†] Giancarlo Terraneo,[*,‡] Pierangelo Metrangolo,[‡,∥] Stuart Brown,[§] and Miguel A. Garcia-Garibay[*,†]

[†]Department of Chemistry and Biochemistry, University of California, Los Angeles, California 90095, United States
[‡]Laboratory of Nanostructured Fluorinated Materials (NFMLab), Department of Chemistry, Materials, and Chemical Engineering "Giulio Natta", Politecnico di Milano, via L. Mancinelli 7, 20131 Milano, Italy
[§]Department of Physics and Astronomy, University of California, Los Angeles, California 90095, United States
[∥]VTT Technical Research Centre of Finland Ltd., Biologinkuja 7, FI-02044 Espoo, Finland

Supporting Information

ABSTRACT: Based on rotational dynamics measurements carried out with isomorphic co-crystals formed by halogen-bonding (XB) between tritylacetylene halides (TrX) and diazabicyclo[2.2.2]octane (dabco), we were able to distinguish the sources of the enthalpic and entropic components in the rotational free energy barrier. We describe the formation of the 1:1 co-crystals ($TrX\cdots N(R)_3N$) obtained from 1 equiv of dabco and 1 equiv of either TrI or TrBr, respectively, to give **4a** and **4b** instead of the potential 2:1 complexes. The co-crystals were prepared by solvent evaporation and mechanochemical synthesis. No co-crystal with TrCl was obtained, reflecting the weaker nature of the $TrCl\cdots NR_3$ interaction. Single-crystal X-ray diffraction confirmed structures that resemble a spinning top on a tripod and revealed that the two XB co-crystals are isomorphous, with slightly different $C-X\cdots NR_3$ (X = I, Br) distances and packing interactions. Quadrupolar-echo ^{2}H NMR experiments with ^{2}H-labeled samples showed that fast rotation of dabco in these co-crystals follows a six-fold potential energy surface with three lowest energy minima. Variable-temperature ^{1}H NMR spin−lattice relaxation (VT ^{1}H T_1) data revealed rotational dynamics with indistinguishable pre-exponential factors and small but distinguishable activation energies. The activation energy of **4b** (E_a = 0.71 kcal mol^{-1}) is the lowest reported in the field of amphidynamic crystals. Using the Eyring equation, we established that their activation entropy for rotation is small but negative ($\Delta S^{\ddagger}$ = −3.0 cal mol^{-1} K^{-1}), while there is almost a 2-fold difference in activation enthalpies, with **4a** having a higher barrier ($\Delta H^{\ddagger}$ = 0.95 kcal mol^{-1}) than **4b** ($\Delta H^{\ddagger}$ = 0.54 kcal mol^{-1}). Analysis of the rotator cavity in the two co-crystals revealed subtle differences in steric interactions that account for their different activation energies.

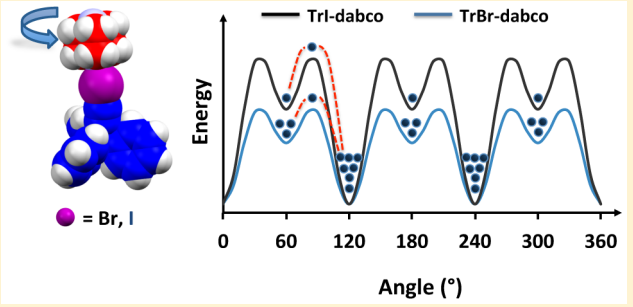

INTRODUCTION

Amphidynamic crystals are materials engineered with a combination of static, lattice-forming components, linked to mobile elements that are able to display rapid and large-amplitude molecular motions.[1] Amphidynamic crystals provide a promising platform for the design of smart functional materials[2] and a distinct approach in the rapidly emergent field of molecular machines.[1,3] We and others have explored the design and dynamics of crystalline molecular rotors[4] by making use of covalent structures,[5] metal coordination,[6] Coulombic interactions,[7] hydrogen bonding,[7b] inclusion compounds,[8] and $\pi-\pi$ stacking.[9] Some of these systems consist of bulky stators, such as trityl (Tr) groups, that create a low-density region for the motion of an axially linked rotator. Another general consideration is that rotators with high axial symmetry order and globular structure tend to have very rapid rotational motion in close-packed crystals as a result of their cylindrical cavities and their small angular displacement between energy minima.[10] Several crystals with ultrafast dynamics have been prepared recently with bicyclo[2.2.2]octane (BCO)[11,12,7b] and 1,4-diazabicyclo-[2.2.2]octane (dabco)[13,14] as rotators.

It has been shown that halogen bonding (XB)[15] is a reliable tool for the realization of crystals displaying fast rotational dynamics[11,13c,14] (Figure 1). For example crystals of bis(1,4-iodoethynyl)bicyclo[2.2.2]octane (BIBCO) **1** exhibit a XB network involving iodine-acetylene interactions.[11] Crystals of **1** display two simultaneous dynamic processes ascribed to two crystallographically distinct BIBCO layers, i.e., an order layer with an activation energy of E_a = 2.75 kcal mol^{-1} and a disordered one with E_a = 1.48 kcal mol^{-1}. We recently reported a supramolecular approach for the preparation of amphidynamic

Received: October 17, 2016
Published: December 19, 2016

DOI: 10.1021/jacs.6b10780
J. Am. Chem. Soc. 2017, 139, 843−848

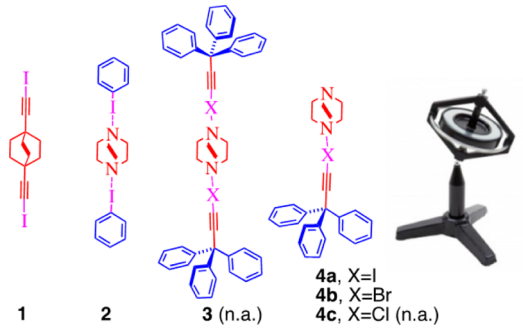

Figure 1. Molecular structures of amphidynamic crystals based on halogen bonding and photograph of the target system, a spinning top on a tripod. Crystals of **1** and **2** were recently reported in the literature. Co-crystals with stator:rotator ratio 2:1 (**3**) and 1:1 (**4a**–**c**) are described in this work. Co-crystals **3** and **4c** were not obtained.

crystals based on the self-assembly of five variously fluorinated iodobenzenes (XB donors) serving as the stators, and dabco (XB acceptor) serving as the supramolecular rotator in co-crystals **2**, which were shown to display activation barriers ranging from 2.4 to 4.9 kcal mol^{-1} (Figure 1).[14]

Considering its modularity and ease of preparation, we decided to explore the XB motif used in **1** (i.e., -C≡C–X, where X is halogen) to target the formation of new supramolecular amphidynamic co-crystals employing a more bulky XB donor, namely the trityl group. As mentioned above, the trityl group is a well-known molecular unit in the construction of molecular rotors that is extensively used as a stator.[16,17] The desired 3,3,3-triphenyl-1-iodopropyne (TrI), 3,3,3-triphenyl-1-bromopropyne (TrBr) or 3,3,3-triphenyl-1-chloropropyne (TrCl) are readily available. The Lewis base diazabicyclo[2.2.2]-octane (dabco) molecule was selected as the XB acceptor because of its average D_{3h} point group symmetry and globular shape, both of which ensure high mobility.[10] Considering the ditopic nature of the dabco rotator,[18] one can recognize that the formation of trimeric (**3**) and dimeric (**4**) adducts could be possible in a crystallization experiment (Figure 1). However, experiments revealed that supramolecular co-crystals of TrI-dabco (**4a**) and TrBr-dabco (**4b**) are readily formed by slow solvent evaporation or by mechanical mixing, while co-crystals of TrCl-dabco (**4c**) could not be obtained. The final stoichiometry of the complexes is independent from the stator:rotator ratios used during the crystallization process.

One of the appealing features of dimer **4** is that substitution of a single halogen atom in an otherwise identical structure is expected to form isomorphous crystals, with subtle packing differences affecting near-neighbor distances, normal modes, and lattice phonons. A priori, one may expect that geometric changes will have an effect on the activation enthalpy while changes in molecular and lattice vibrations should have an effect on the activation entropy. As described in detail below, variable-temperature ^{2}H line shape analysis and ^{1}H T_1 spin–lattice relaxation measurements revealed ultrafast dabco rotation in a 6-fold potential with the two co-crystals having the same activation entropy ($\Delta S^{\ddagger}$) but clearly distinguishable activation enthalpies ($\Delta H^{\ddagger}$).

RESULTS AND DISCUSSION

Samples of iodo-, bromo-, and chlorotritylacetylene XB donors were prepared as reported in the literature (see Supporting Information (SI)). Co-crystallizations were carried out by slow evaporation from acetone solutions of the corresponding trityl halide and dabco. While several conditions afforded good quality co-crystals containing TrI (**4a**) or TrBr (**4b**) and dabco, no co-crystals were formed with TrCl (**4c**). The behavior of TrCl molecule was expected and could be explained by the poor XB donor ability of chlorine.[19] It is known that the interaction strength of a XB contact is strictly correlated to the polarizability of the halogen atom involved in the interaction.[20] Chlorine is less polarizable than iodine or bromine and thus its halogen bond with the "rotating" dabco is very weak, so weak that is not able to drive the formation of the target co-crystal.

Co-crystals **4a** and **4b** were diffracted at 100 K and at 298 K and their crystal structures were solved in the monoclinic space group $P2_1/c$ at both temperatures, and a detailed comparison demonstrated their isomorphic relationship. The expected supramolecular complexes engage the I and Br atoms of TrX and one nitrogen atom of dabco (C–X···NR$_3$) in halogen bonding (XB) in a way that they resemble supramolecular spinning tops on a tripod (Figure 2a). As anticipated, the XB

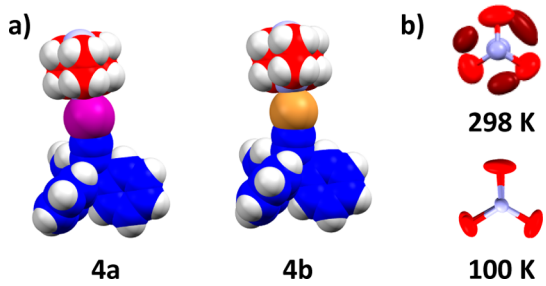

Figure 2. (a) Structures of co-crystals **4a** and **4b** obtained at 100 K and (b) a top-down view along the N–N axis of dabco within **4a** crystal lattice at 298 K and at 100 K displaying the presence and absence of disorder, respectively. At 298 K the two splitted positions of the dabco alkyl chains are highlighted in red (0.69 occupancy) and red brick (0.31 occupancy). Color code: stator C, blue; rotator C, red and red brick; N, light blue; H, white; I, magenta; Br, orange.

interaction in **4a** is stronger and more linear than in complex **4b** as demonstrated by shorter N···X contacts and N···X–C angles that are closer to the ideal 180° (see Table 1).

Table 1. Geometrical Features Present in Co-crystals 4a and 4b at Two Different Temperatures

complex	N···X (N_C)[a]	N···X–C angle (deg)
4a (298 K)	0.78	175.21 (7)
4a (100 K)	0.78	173.88 (9)
4b (298 K)	0.83	173.73 (8)
4b (100 K)	0.82	172.17 (6)

[a]XB distances are expressed as normalized contacts (N_C) according to ref 15.

One of the most interesting features in the structure of co-crystals **4a** and **4b** is that the molecular structure of dabco at 100 K does not present disorder, while the structure solution at 298 K requires two positions with occupancies of 69:31 in **4a** and 62:38 in **4b** (Figure 2b and Table S2 in the SI). It is worth noting that the TrX stators are not disordered at these two temperatures. The disorder of dabco was interpreted and later on confirmed to be dynamic in nature. From analysis of the atomic displacement parameters (ADPs), one can also infer that rotation occurs along the N–N axis of dabco, as the

DOI: 10.1021/jacs.6b10780
J. Am. Chem. Soc. 2017, 139, 843–848

ADPs display elongations on the plane perpendicular to the rotational axis.

The crystal packings of **4a** and **4b** can be described as pairs of columns of dabco and TrX molecules that propagate in the direction of the *a* axis by translation along the same axis and a 180° rotation along the *b* axis that runs parallel to the column (Figure 3). It is interesting to observe that the trityl halide

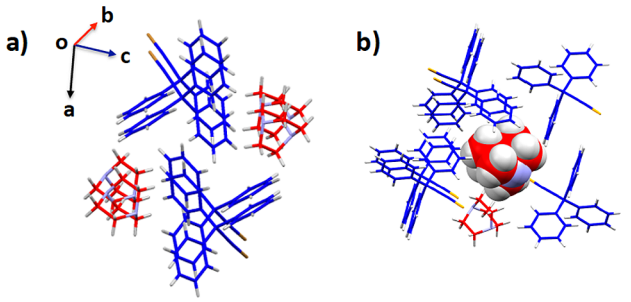

Figure 3. (a) Columnar arrays of TrBr and dabco molecules in the structure of co-crystal **4b** and (b) a dabco rotator in a cavity surrounded by six molecules of TrBr and one dabco.

molecules, within the column and with adjacent columns, are engaged in edge-to-face interactions.[17] Two adjacent columns of dabco molecules sit in cavities composed of three adjacent trityl halide columns (Figure 3), which generate some free volume around the rotator. A parameter indirectly related to this free volume is the packing coefficient (C_k), defined as the ratio between the van der Waals volume of the molecules in the unit cell in relation to the total volume of the unit cell.[1b,21] Interestingly, the packing coefficients for **4a** and **4b** are exactly the same, $C_k = 0.66$ at 100 K, which in the context of molecular crystals is quite small (ca. $C_k = 0.65–0.77$)[1b,21] and comparable to crystalline molecular rotors showing high dynamics (C_k = 0.68[22a] and 0.69[22b,c]). Another sign of the structural and dynamic similarities between the two co-crystals comes from their nearly identical IR spectra (see SI), which provide information related to normal modes and lattice phonons, which may be expected to result in similar rotational dynamics.

Pure phase crystalline bulk materials of **4a** and **4b** were also obtained by solvent assisted mechanochemical crystallization.[23] The crystalline phases of the bulk materials were analyzed by powder X-ray diffraction analysis, which showed that the patterns of **4a** and **4b** matched the calculated patterns from the single-crystal X-ray diffraction analyses and were congruent between them; this confirmed that these materials are isomorphic. The thermal stabilities of both materials were determined by melting point, thermal gravimetric analysis (TGA) and differential scanning calorimetry (DSC). Visual melting point analyses showed that **4a** and **4b** co-crystals melt with decomposition in the ranges of 140–146 °C and 157–160 °C, respectively. Additionally, TGA and DSC analyses showed that both samples start to decompose before melting at ca. 120 °C.

With crystallographic and thermal stability information available we were able to evaluate the dynamic performance of isomorphic co-crystals **4a** and **4b**. As a first glance into the dynamics of dabco, we decided to use quadrupolar-echo ^{2}H NMR, as the line shape of the spectra are sensitive to the magnitude and rate of the angular displacement of the mobile element resulting from the dynamic modulation of electric field gradient (EFG) interaction with the electric quadrupole moment (eQ) in the C–D bond.[24] Simulation of the ^{2}H spectrum provides the site exchange rate and the jump angle.[24b] With this in mind, we prepared a sample of **4b** with isotopically enriched dabco-d_{12} (**4b**-d_{12}). Quadrupolar-echo ^{2}H NMR experiments were recorded at 46.2 MHz and at 296 K, 210 K, and 150 K, with the latter being the lowest temperature attainable with our instrument. Comparison of the three spectra showed no significant line-shape differences. All three spectra were satisfactorily simulated using a model that considers either 120° or 60° jump angles (see SI) in the fast exchange limit of 10^8 s^{-1}. This result is in agreement with the dynamic disorder and thermal ellipsoids of the dabco rotator observed in the single-crystal X-ray structure. It should also be pointed out that in the fast exchange regime there is no difference in line shape between 3-fold (120°) and 6-fold (60°) rotational symmetry orders.

In order to calculate the activation parameters (E_a, τ_0^{-1}, $\Delta H^{\ddagger}$, $\Delta S^{\ddagger}$) for the rotation of dabco rotator in the XB co-crystals, **4a** and **4b**, we needed a probe that covers a larger dynamic range. In this scenario, we turned our attention to ^{1}H spin–lattice relaxation (^{1}H T_1). This technique is ideal for the characterization of dynamic processes that modulate magnetic interactions near the Larmor frequency ($\omega_0 = 2\pi\nu_0$) of the observed nucleus.[4a] For a thermally activated process, i.e., dabco rotation, that takes place with a correlation time (τ_c), its dependence with the temperature is given by the Arrhenius (eq 1) and the Eyring (eq 2) equations. On the other hand, the dependence of the characteristic time constant T_1 for the recovery of the magnetization on the *z* axis with τ_c is given by the Kubo–Tomita equation[25] (eq 3). Therefore, the behavior of experimental T_1 data as a function of the temperature can be described combining eqs 1 and 2 with eq 3. Even though eq 3 is valid for isotropic motions, it describes well the relaxation in powdered crystalline samples where a random distribution of rotational axes makes it possible to apply an averaging procedure. Additionally, efficient spin diffusion and simple and well-defined dynamic processes where the relaxation is dominated by intramolecular dipolar interactions make it possible to employ eq 3.[25c]

$$\tau_c = \tau_0 \exp(E_a/RT) \quad (1)$$

$$\tau_c = h/k_B T \exp(-\Delta S^{\ddagger}/R) \exp(\Delta H^{\ddagger}/RT) \quad (2)$$

$$T_1^{-1} = C[\tau_c(1 + \omega_0^2\tau_c^2)^{-1} + 4\tau_c(1 + 4\omega_0^2\tau_c^2)^{-1}] \quad (3)$$

$$C = (n/N)(9/40)(\mu_0/4\pi)^2\gamma^4\hbar^2/r^6 \quad (4)$$

In the Arrhenius equation, τ_0 (eq 1) represents the inverse of the attempt frequency. In the Kubo–Tomita equation (eq 3), the constant C (eq 4) represents the strength of the dipolar interactions involved in the relaxation process, which depends on the ratio of the mobile nuclei responsible for the relaxation (n) to the total number of nuclei that need to be relaxed (N), μ_0 is the permeability of free space, γ is the gyromagnetic ratio, $\hbar$ is the reduced Plank constant, and r is the internuclei distance.

Using microcrystalline samples of **4a** and **4b** we performed variable-temperature ^{1}H T_1 experiments at a frequency $\nu_0 = \omega_0/2\pi$ of 359.9 MHz for proton and a saturation recovery pulse sequence. Individual relaxation curves were properly described by single exponential functions (see SI). Experiments with **4a** were recorded in the range of 80–165 K with a minimum in T_1 found at 100 K. In the case of **4b**, ^{1}H T_1 experiments were

DOI: 10.1021/jacs.6b10780
J. Am. Chem. Soc. 2017, 139, 843–848

recorded in the range of 40−155 K presenting a minimum in T_1 at 65 K (see SI). Although crystal X-ray diffraction data at room temperature and quadrupolar-echo ^{2}H NMR experiments suggested 3-fold and 6-fold rotations, only one relaxation mechanism was observed. Considering that the corresponding trajectories are not independent, it seems reasonable that the slower 3-fold rotation is relaxation rate-limiting at the temperatures studied. An excellent fit of the experimental relaxation data (T_1) to the Kubo−Tomita equation[25] was obtained with the data presented in Table 2 (Figure 4). Given the fact that the

Table 2. Activation Parameters for the Rotation of dabco in Co-crystals 4a (TrI-dabco) and 4b (TrBr-dabco)

	4a	4b
space group (Z)	$P2_1/c$ (4)	$P2_1/c$ (4)
E_a (kcal mol^{-1})	1.15 ± 0.04	0.71 ± 0.04
τ_0^{-1} (×10^{12} s^{-1})	1.3 ± 0.3	1.2 ± 0.4
C (×10^9 s^{-2})	2.55 ± 0.4	2.6 ± 0.7
$\Delta H^{\ddagger}$ (kcal mol^{-1})	0.95 ± 0.06	0.54 ± 0.06
$\Delta S^{\ddagger}$ (cal mol^{-1} K^{-1})	−3.0 ± 0.7	−3.0 ± 0.8

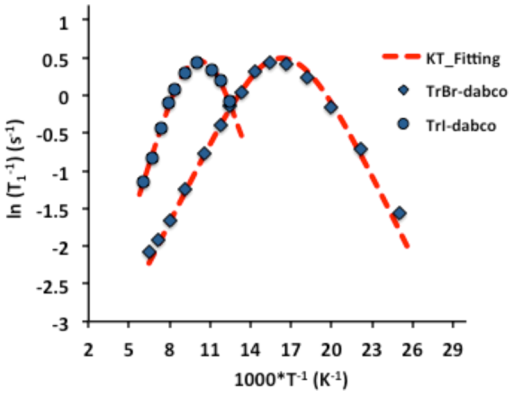

Figure 4. ^{1}H T_1 experiments as a function of the temperature plotted as ln (T_1^{-1}) vs 1000*T^{-1}. ^{1}H T_1 was measured at 359.9 MHz in the range of 80−165 K and 40−155 K on co-crystals **4a** (solid circles) and **4b** (solid diamonds), respectively. ^{1}H T_1 Minima occurred at approximately 100 K for **4a** and 65 K for **4b**. The red dotted lines correspond to the Kubo−Tomita fittings of the experimental data.

crystal structures of **4a** and **4b** are isomorphic, it is interesting to observe that there are almost no differences in the C constants and pre-exponential factors (τ_0^{-1}), although they have small but clearly distinguishable energy barriers. As expected for structures with the same number of protons involved in the relaxation mechanism, the C constant for both co-crystals has almost the same value, 2.55(±0.4) × 10^9 and 2.6(±0.7) × 10^9 s^{-2} for **4a** and **4b**, respectively (Table 2). Related to the frequency of torsional oscillations of the dabco rotator within its potential energy well, we found that the pre-exponential factors (τ_0^{-1}) are almost the same for the two halogen bonbed co-crystals, 1.3(±0.3) × 10^{12} and 1.2(±0.4) × 10^{12} s^{-1}. This observation is in line with a mechanism where normal modes and lattice phonons combine to produce essentially identical librations, as expected for the isomorphic crystal structures. However, we found an activation energy of E_a = 0.71(±0.04) kcal mol^{-1} for **4b**, which is 38% lower as compared to the E_a = 1.15(±0.04) kcal mol^{-1} of **4a**, with the former being the lowest reported in the field of amphidynamic crystals. We propose that such a low activation energies are in line with the low packing coefficients of **4a** and **4b** co-crystals, C_k = 0.66, which means that the crystals are loosely packed and have enough empty space for the rotation of dabco. We propose that in isomorphic crystal structures **4a** and **4b**, with the only difference being the strength of the C−X···NR$_3$ interaction, the small differences in E_a could come from small differences in the cavity of the rotator. As previously noted, the strength of the XB is reflected in the length and directionality of the C−X···NR$_3$ interaction, where, as predicted, this distance is shorter in **4a** than in **4b**. As a consequence, we could foresee that the dabco makes different contacts with the neighboring molecules. We found that, as a result of dabco being closer to the iodine atom, the close contact interactions of the unbound nitrogen with two hydrogen atoms of two different TrX molecules are longer (2.71 Å, 2.91 Å) in **4a** as compared to the same ones in **4b** (2.68 Å, 2.88 Å) (Figure 5). Furthermore, in

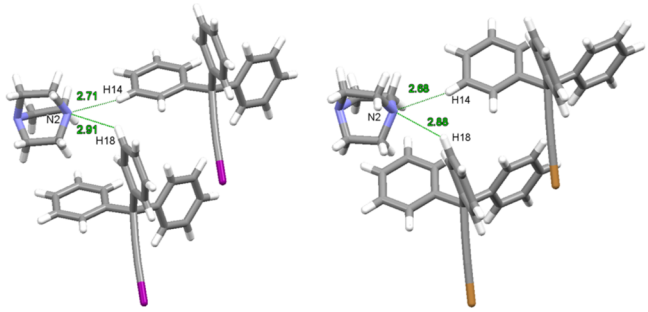

Figure 5. Close up of the crystal structures of **4a** (left) and **4b** (right) where weak hydrogen bonds between the unbound nitrogen and two different aromatic hydrogen atoms are highlighted. Contacts and distances (in Å) are in green. Color code: C, gray; N, light blue; H, white; I, magenta; Br, orange.

the more loosely bound co-crystal **4b** the rotator alkyl chains present longer close contact interactions with neighboring aryl groups than those in **4a**. We found that the rotator cavity is larger in **4b** than in **4a**, 169.6 Å^3 and 162.8 Å^3, respectively at 100 K. We reasoned that smaller rotator cavity creates a more crowded environment for the rotation of dabco in **4a**, thus raising the activation energy.

We reasoned that the thermodynamic parameters of activation, enthalpy ($\Delta H^{\ddagger}$) and entropy ($\Delta S^{\ddagger}$), would reflect these steric interactions. As expected from their similar pre-exponential factor, rotation of dabco in crystals of **4a** and **4b** takes place with the same activation entropy, $\Delta S^{\ddagger}$ = −3.0 cal mol^{-1} K^{-1}. A relatively small but negative value suggests that lattice vibrations correlate to generate a highly ordered transition state for dabco to jump from one energy well to the other. On the other hand, we observed that $\Delta H^{\ddagger}$ in **4a** is almost twice as large, 0.95 ± 0.06 kcal mol^{-1}, as that of **4b**, 0.54 ± 0.06 kcal mol^{-1}, suggesting that relatively subtle differences in steric interactions are responsible for the higher enthalpic barrier of **4b**.

Based on crystallographic data, quadrupolar-echo ^{2}H NMR and activation parameters (E_a, τ_0^{-1}, $\Delta H^{\ddagger}$ and $\Delta S^{\ddagger}$) obtained by ^{1}H T_1 relaxometry experiments, we proposed a 6-fold potential energy surface with three lowest energy minima. We inferred by crystallographic data that the second equilibrium position observed by X-ray diffraction analysis is of lower activation energy and occurs at a higher potential energy level, which explains why it is the less populated at low temperatures (Figure 6). The potential energy surface diagram also shows that the rotational barrier for dabco in **4b** is lower than in **4a**.

DOI: 10.1021/jacs.6b10780
J. Am. Chem. Soc. 2017, 139, 843−848

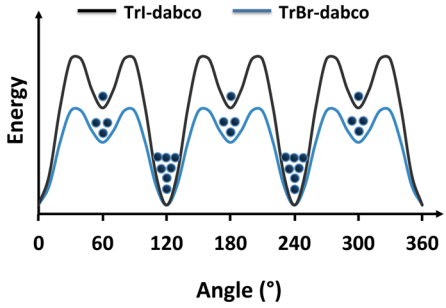

Figure 6. Potential energy surface for the rotation of dabco in co-crystals of **4a** (black trace) and **4b** (blue trace).

CONCLUSIONS

We have successfully designed and realized two new halogen-bonded supramolecular spinning tops on a tripod, **4a** and **4b**, which show isomorphic crystal structures at 100 K and room temperature. In agreement with the strength of the halogen bonding, we observed that the C–X···NR_3 distance is shorter when iodine is present, as in the case of **4a**, as compared to the case when a bromine atom is the XB donor in **4b**. Solvent-assisted mechanochemical crystallization allowed us to prepare pure crystalline phase samples of **4a** and **4b**, which were evaluated by ^{1}H T_1 relaxometry experiments. We observed a good correlation between their loose crystal packing, C_k = 0.66 at 100 K, and the small barriers of 1.15(±0.04) and 0.71(±0.04) kcal mol^{-1}, respectively, for dabco rotation in co-crystals **4a** and **4b**. It was also shown that pre-exponential factors for dabco rotation in **4a** and **4b** are almost identical, with values of τ_0^{-1} = 1.3(±0.3) × 10^{12} and 1.2(±0.4) × 10^{12} s^{-2}, respectively. Taking advantage of isomorphic co-crystals with nearly identical crystal structures with similar normal vibrational modes and lattice phonons we were able to sort out the origin of the enthalpy and entropy of activation. Accordingly, fitting ^{1}H T_1 data to the Eyring and Kubo-Tomita equations, we unveiled essentially identical negative activation entropies ($\Delta S^{\ddagger}$ = −3.0 cal mol^{-1} K^{-1}) and clearly distinguishable activation enthalpies. Thus, the enthalpic barrier for dabco rotation in co-crystal **4a** ($\Delta H^{\ddagger}$ = 0.95 ± 0.06 kcal mol^{-1}) is almost twice as large as that of **4b** ($\Delta H^{\ddagger}$ = 0.54 ± 0.06 kcal mol^{-1}). This difference can be assigned to subtle differences in their crystal structures, which result in a more hindered environment for the dabco cavity in **4a**.

ASSOCIATED CONTENT

Supporting Information

The Supporting Information is available free of charge on the ACS Publications website at DOI: 10.1021/jacs.6b10780.

Preparation and characterization of halogen-bonded co-crystals, spectroscopic data, and supporting experiments (PDF)

X-ray crystallographic data for **4a** at 100 K (CIF)

X-ray crystallographic data for **4a** at 298 K (CIF)

X-ray crystallographic data for **4b** at 100 K (CIF)

X-ray crystallographic data for **4b** at 296 K (CIF)

AUTHOR INFORMATION

Corresponding Authors

*giancarlo.terraneo@polimi.it

* mgg@chem.ucla.edu

ORCID

Luca Catalano: 0000-0002-1003-6512

Miguel A. Garcia-Garibay: 0000-0002-6268-1943

Notes

The authors declare no competing financial interest.

ACKNOWLEDGMENTS

This work was supported by National Science Foundation Grants DMR140268 (M.A.G.-G.) and DMR-1410343 (S.B.) and by the Italian Ministry of University and Research, grant PRIN 2010-2011 no. 2010ERFKXL (P.M. and G.T.).

REFERENCES

(1) (a) Garcia-Garibay, M. A. *Proc. Natl. Acad. Sci. U. S. A.* **2005**, *102*, 10771–10776. (b) Vogelsberg, C. S.; Garcia-Garibay, M. A. *Chem. Soc. Rev.* **2012**, *41*, 1892–1910.

(2) (a) Setaka, W.; Yamaguchi, K. *Proc. Natl. Acad. Sci. U. S. A.* **2012**, *109*, 9271–9275. (b) Setaka, W.; Yamaguchi, K. *J. Am. Chem. Soc.* **2012**, *134*, 12458–12461.

(3) (a) Cheng, C.; Stoddart, J. F. *ChemPhysChem* **2016**, *17*, 1780–1793. (b) Coskun, A.; Banaszak, M.; Astumian, R. D.; Stoddart, J. F.; Grzybowski, B. A. *Chem. Soc. Rev.* **2012**, *41*, 19–30. (c) Szymanski, W.; Beierle, J. M.; Kistemaker, H. A. V.; Velema, W. A.; Feringa, B. L. *Chem. Rev.* **2013**, *113*, 6114–6178. (d) Feringa, B. L.; van Delden, R. A.; Koumura, N.; Geertsema, E. M. *Chem. Rev.* **2000**, *100*, 1789–1816. (e) Feringa, B. L. *Acc. Chem. Res.* **2001**, *34*, 504–513. (f) Sauvage, J. P. *Acc. Chem. Res.* **1998**, *31*, 611–619. (g) Collin, J.-P.; Dietrich-Buchecker, C.; Gavina, P.; Jimenez-Molero, M. C.; Sauvage, J.-P. *Acc. Chem. Res.* **2001**, *34*, 477–487. (h) Erbas-Cakmak, S.; Leigh, D. A.; McTernan, C. T.; Nussbaumer, A. L. *Chem. Rev.* **2015**, *115*, 10081–10206.

(4) (a) Kottas, G. S.; Clarke, L. I.; Horinek, D.; Michl, J. *Chem. Rev.* **2005**, *105*, 1281–1376. (b) Akutagawa, T.; Koshinaka, H.; Sato, D.; Takeda, S.; Noro, S.-I.; Takahashi, H.; Kumai, R.; Tokura, Y.; Nakamura, T. *Nat. Mater.* **2009**, *8*, 342–347. (c) Commins, P.; Garcia-Garibay, M. A. *J. Org. Chem.* **2014**, *79*, 1611–1619. (d) Comotti, A.; Bracco, S.; Yamamoto, A.; Beretta, M.; Hirukawa, T.; Tohnai, N.; Miyata, M.; Sozzani, P. *J. Am. Chem. Soc.* **2014**, *136*, 618–621.

(5) (a) Khuong, T.-A. V.; Nuñez, J. E.; Godinez, C. E.; Garcia-Garibay, M. A. *Acc. Chem. Res.* **2006**, *39*, 413–422. (b) Karlen, S. D.; Garcia-Garibay, M. A. *Topics Curr. Chem.* **2006**, *262*, 179–228.

(6) (a) Torres-Huerta, A.; Rodríguez-Molina, B.; Höpfl, H.; Garcia-Garibay, M. A. *Organometallics* **2014**, *33*, 354–362. (b) Gould, S. L.; Tranchemontagne, D.; Yaghi, O. M.; Garcia-Garibay, M. A. *J. Am. Chem. Soc.* **2008**, *130*, 3246–3247.

(7) (a) Comotti, A.; Bracco, S.; Yamamoto, A.; Beretta, M.; Hirukawa, T.; Tohnai, N.; Miyata, M.; Sozzani, P. *J. Am. Chem. Soc.* **2014**, *136*, 618–621. (b) Lemouchi, C.; Mézière, C.; Zorina, L.; Simonov, S.; Rodríguez-Fortea, A.; Canadell, E.; Wzietek, P.; Auban-Senzier, P.; Pasquier, C.; Giamarchi, T.; Garcia-Garibay, M. A.; Batail, P. *J. Am. Chem. Soc.* **2012**, *134*, 7880–7891.

(8) Kobr, L.; Zhao, K.; Shen, Y.; Comotti, A.; Bracco, S.; Shoemaker, R. K.; Sozzani, P.; Clark, N. A.; Price, J. C.; Rogers, C. T.; Michl, J. *J. Am. Chem. Soc.* **2012**, *134*, 10122–10131.

(9) Harada, J.; Ohtani, M.; Takahashi, Y.; Inabe, T. *J. Am. Chem. Soc.* **2015**, *137*, 4477–4486.

(10) Karlen, S. D.; Reyes, H.; Taylor, R. E.; Khan, S. I.; Hawthorne, M. F.; Garcia-Garibay, M. A. *Proc. Natl. Acad. Sci. U. S. A.* **2010**, *107*, 14973–14977.

(11) Lemouchi, C.; Vogelsberg, C. S.; Zorina, L.; Simonov, S.; Batail, P.; Brown, S.; Garcia-Garibay, M. A. *J. Am. Chem. Soc.* **2011**, *133*, 6371–6379.

(12) (a) Lemouchi, C.; Iliopoulos, K.; Zorina, L.; Simonov, S.; Wzietek, P.; Cauchy, T.; Rodríguez-Fortea, A.; Canadell, E.; Kaleta, J.; Michl, J.; Gindre, D.; Chrysos, M.; Batail, P. *J. Am. Chem. Soc.* **2013**, *135*, 9366–9376. (b) Rodríguez-Molina, B.; Pérez-Estrada, S.; Garcia-Garibay, M. A. *J. Am. Chem. Soc.* **2013**, *135*, 10388–10395. (c) Lemouchi, C.; Yamamoto, H. M.; Kato, R.; Simonov, S.; Zorina, S.; Rodríguez-Fortea, A.; Canadell, E.; Wzietek, P.; Iliopoulos, K.;

DOI: 10.1021/jacs.6b10780
J. Am. Chem. Soc. 2017, 139, 843–848

Gindre, D.; Chrysos, M.; Batail, P. *Cryst. Growth Des.* **2014**, *14*, 3375−3383.
(13) (a) Zhang, Y.; Zhang, W.; Li, S.-H.; Ye, Q.; Cai, H.-L.; Deng, F.; Xiong, R.-G.; Huang, S. D. *J. Am. Chem. Soc.* **2012**, *134*, 11044−11049. (b) Gabuda, S. P.; Kozlova, S. G.; Samsonenko, D. G.; Dybtsev, D. N.; Fedin, V. P. *J. Phys. Chem. C* **2011**, *115*, 20460−20465.
(14) Catalano, L.; Pérez-Estrada, S.; Terraneo, G.; Pilati, T.; Resnati, G.; Metrangolo, P.; Garcia-Garibay, M. A. *J. Am. Chem. Soc.* **2015**, *137*, 15386−15389.
(15) Cavallo, G.; Metrangolo, P.; Milani, R.; Pilati, T.; Priimagi, A.; Resnati, G.; Terraneo, G. *Chem. Rev.* **2016**, *116*, 2478−2601.
(16) (a) Arcos-Ramos, R.; Rodriguez-Molina, B.; Gonzalez-Rodriguez, E.; Ramirez-Montes, P. I.; Ochoa, M. E.; Santillan, R.; Farfán, N.; Garcia-Garibay, M. A. *RSC Adv.* **2015**, *5*, 55201−55208. (b) Dominguez, Z.; Dang, H.; Strouse, M. J.; Garcia-Garibay, M. A. *J. Am. Chem. Soc.* **2002**, *124*, 7719−7727. (c) Dominguez, Z.; Khuong, T.-A. V.; Dang, H.; Sanrame, C. N.; Nunez, J. E.; Garcia-Garibay, M. A. *J. Am. Chem. Soc.* **2003**, *125*, 8827−8837.
(17) Stopin, A.; Garcia-Garibay, M. A. *Cryst. Growth Des.* **2012**, *12*, 3792−3798.
(18) (a) Messina, M. T.; Metrangolo, P.; Navarrini, W.; Radice, S.; Resnati, G.; Zerbi, G. *J. Mol. Struct.* **2000**, *524*, 87−94. (b) Cincic, D.; Friscic, T.; Jones, W. *Chem. - Eur. J.* **2008**, *14*, 747−753. (c) Perkins, C.; Libri, S.; Adams, H.; Brammer, L. *CrystEngComm* **2012**, *14*, 3033−3038. (d) Brisdon, A. K.; Muneer, A. M. T.; Pritchard, R. G. *Acta Crystallogr., Sect. C: Struct. Chem.* **2015**, *71*, 900−902.
(19) Clark, T.; Hennemann, M.; Murray, J. S.; Politzer, P. *J. Mol. Model.* **2007**, *13*, 291−296.
(20) (a) Riley, K. E.; Murray, J. S.; Fanfrlík, J.; Řezáč, J.; Solá, R. J.; Concha, M. C.; Ramos, F. M.; Politzer, P. *J. Mol. Model.* **2011**, *17*, 3309−3318. (b) Politzer, P.; Murray, J. S.; Lane, P.; Concha, M. C. *Int. J. Quantum Chem.* **2009**, *109*, 3773−3780.
(21) (a) Kitaigorodsky, A. I. *Molecular Crystals and Molecules*; Academic Press: New York, 1973. (b) O'Brien, Z. J.; Natarajan, A.; Khan, S.; Garcia-Garibay, M. A. *Cryst. Growth Des.* **2011**, *11*, 2654−2659.
(22) (a) Khuong, T.-A. V.; Zepeda, G.; Ruiz, R.; Khan, S. I.; Garcia-Garibay, M. A. *Cryst. Growth Des.* **2004**, *4*, 15−18. (b) Godinez, C. E.; Zepeda, G.; Mortko, C. J.; Dang, H.; Garcia-Garibay, M. A. *J. Org. Chem.* **2004**, *69*, 1652−1662. (c) Godinez, C. E.; Garcia-Garibay, M. A. *Cryst. Growth Des.* **2009**, *9*, 3124−3128.
(23) Braga, D.; Maini, L.; Grepioni, F. *Chem. Soc. Rev.* **2013**, *42*, 7638−7648.
(24) (a) Fyfe, C. A. *Solid State NMR for Chemists*; CFC Press: Guelph, Ontario, 1983. (b) Nishikiori, S. I.; Soma, T.; Iwamoto, T. *J. Inclusion Phenom. Mol. Recognit. Chem.* **1997**, *27*, 233−243.
(25) (a) Kubo, R.; Tomita, K. *J. Phys. Soc. Jpn.* **1954**, *9*, 888−919. (b) Bakhmutov, V. I. *Practical NMR Relaxation for Chemists*; John Wiley & Sons Ltd: Chichester, England, 2004. (c) Conn, K. G.; Beckmann, P. A.; Mallory, C. W.; Mallory, F. B. *J. Chem. Phys.* **1987**, *87*, 20−27.

DOI: 10.1021/jacs.6b10780
J. Am. Chem. Soc. 2017, 139, 843−848